Vol. 46, No. 4 (2024) 560-569, DOI: 10.24874/ti.1642.03.24.05

Tribology in Industry

www.tribology.rs

RESEARCH

Effect of Electrode Material Variations on Wear Characteristics of Stir Cast A356/Red Mud/TiC Hybrid Metal Matrix Composite During Electrical Discharge Machining

Debasmita Pani[a], B. Surekha[b], Rishitosh Ranjan[b], Priyaranjan Samal[c], S. Rama Rao[d], Prakash Chandra Mishra[e,*]

[a]*Department of Mechanical Engineering, Indian Institute of Technology, Jodhpur, Rajasthan-342030, India,*
[b]*School of Mechanical Engineering, KIIT(DU), Bhubaneswar 751024, India,*
[c]*Department of Mechanical Engineering, Koneru Lakshmaiah Education Foundation, Vaddeswaram, A.P 522302, India,*
[d]*Department of Mechanical Engg, Tirumala Engineering College, Narasaraopet 522601, India*
[e]*Department of Mechanical Engineering, Veer Surendra Sai University of Technology Burla 768108, India.*

Keywords:

Aluminium alloy
Red mud
TiC
Material removal rate
Tool wear rate
Surface roughness

* Corresponding author:

Prakash Chandra Mishra
E-mail: prabasmishra73@gmail.com

Received: 13 March 2024
Revised: 20 April 2024
Accepted: 27 May 2024

A B S T R A C T

In the current study, an aluminum alloy A356-based hybrid metal matrix composite with red mud and titanium carbide reinforcements is fabricated using a liquid processing route namely the stir casting method. The machining characteristics along with the suitable electrode material during the electric discharge machining of the fabricated composite are determined. The authors are interested in studying the effects of various electric discharge machining (EDM) input parameters like peak current, the voltage on time, and gap voltage affecting the material removal rate (MRR) and tool wear rate (TWR) at the time of machining. Levels of input parameters to conduct the experiments are considered from the literature review, machine capacity, and pilot experiments. To predict the suitable electrode material for the newly fabricated heterogeneous composite material, different electrode materials namely brass, copper, graphite, and stainless steel are used to perform the experiments. Further, the surface roughness of the machined surface is measured and compared for different electrode materials used in the present work. From the results, it has been observed that copper electrode followed by stainless steel electrode show the least tool wear rate (TWR), while brass exhibited the highest TWR. Stainless steel electrode has shown a 90.73% reduction in TWR when compared with brass which has shown the largest TWR. But the Graphite electrode had shown a 57.19% improvement in MRR when compared with stainless steel which had produced a lower value of MRR.

1. INTRODUCTION

With technological advancement and demand for innovative applications, the requirement for specific materials has risen. Metal matrix composites are being utilized as a chief group of building materials for automotive, defense, and aerospace applications because of their low density, high specific strength, and high specific modulus, along with the higher service temperatures. Moreover, compared to monolithic materials, MMCs are reported to depict better physical, mechanical, and wear properties [1]. Ceramic particles have been a compelling choice as reinforcements in metal matrices. Previously, titanium carbide TiC, titanium boride TiB, titanium diboride TiB_2, and silicon carbide SiC have been incorporated as reinforcements in different MMCs. Amongst these ceramic reinforcements, TiC is considered a fascinating one due to its enhanced thermal stability, better chemical compatibility, better resistance to corrosion and oxidation in unfavorable environments, and mechanical properties that include very high hardness and high elastic modulus [2-5].

Xianglong Sun et al. [2] Synthesized composites with in-situ TiC and MWCNTs reinforcements in the Ti matrix through vacuum hot press sintering and hot rolling process. They reported that the proportion and particle size of TiC increased with MWCNTs proportion resulting in the formation of different microstructure and grain refinement after rolling deformation. Grain refinement, solid solution strengthening of C, and dispersion strengthening in TiC significantly increased the strength and hardness of the composite. H.A.Rastegari et al [6] fabricated composites with TiC reinforcements and Ti-6Al-4V matrix in graphite crucible by vacuum induction melting (VIM) method forming Grain boundary, eutectic and trans granular TiC precipitates. They reported that compared to neat Ti-6Al-4V, TiC-reinforced composites showed greater hardness and tensile strength which further increased with volume fraction of TiC. Several metallurgical processes such as liquid-based stir casting process [7,8], powder-based technique[9,10], semi-solid powder densification [11], pellet method [12], and spray automation and deposition [13] are being adopted by the researchers for the fabrication of MMCs.

Amongst all these, liquid phase stir casting has been the foremost economical and simplest route for the fabrication of metal matrix composites commercially [14,15]. Kalaiselvan et al. [16] prepared boron carbide-reinforced Al alloy composites using different techniques like squeeze casting, stir casting, spray deposition, pressure infiltration, liquid infiltration, and powder metallurgy and studied their characterization. Stir casting is a relatively cheap manufacturing process that additionally provides a wide selection of materials. Belete et al [17] prepared and studied ceramic particle-reinforced Al composites using stir casting. They reported that the stir casting route is a simple and cost-effective method of composite fabrication that assists in better particle dispersion in the metal matrix while stirring. Johny et al. [18] applied the stir casting method to fabricate Al6061 and $ZrSiO_4$ composites and identified homogeneous microstructure within the developed specimens. Müller and J. Monaghan [19] studied aluminum matrix composite manufactured by the method of stir casting process is having improved mechanical properties.

The greatest drawback related to MMCs is their high price. Therefore, currently, the emphasis is on manufacturing composites that incorporate reinforcements that are relatively cheap and have low density. Materials like graphite, fly ash, red mud, etc. are obtainable reinforcements for MMCs. Amongst these, red mud, obtained in massive quantities during extraction of aluminum from bauxite ore is an economical as well as low-density alternative for particulate reinforcements in composites that can be utilized for automotive applications**.** Ravi C Naikar [20] prepared uniformly distributed red mud (3 wt%, 6 wt%, 9 wt%) reinforced aluminum matrix composite through stir casting and studied its mechanical properties. The work reported that the wear rate increases with the weight percentage of red mud while the tensile strength increases with the weight percentage of red mud up to 6% after which it decreases. Amit Sharma et al [21] fabricated Al-2014/Red mud metal matrix composites with 5 wt% to 15 wt% of reinforcements using 90μ and 150μ particle sizes. It was concluded from findings that tensile strength and hardness improved with weight percentage of red mud and maximum was obtained at 15 wt% and 90μm grain size.

Electric discharge machining is one of the earliest non-traditional machining processes. Electric-discharge machining was invented by Russian engineers, B.R. Lazarenko and N.I. Lazarenko in 1943. Though electro-discharge machining is limited to only electrically conductive tool and workpiece, it allows for very high surface finish rates with no mechanical vibrations and mechanical stresses occurring during machining as there is no physical contact between tool and workpiece [22]. F. Müller et al [23] studied A356 reinforced SiC (35% and 13µm grain size) composites fabricated through a powder metallurgy route involving Hot-Isostatic Pressing (HIP). The results obtained showed that the prepared MMC can be machined using electro-discharge machining which is otherwise difficult to machine using conventional machining processes as SiC particle-reinforced Al matrix composites cause excessive tool wear. However, the material removal rate reported was low compared to the conventional machining process. Also, the Cu electrode was found to be more effective than the graphite electrode. During electric-discharge machining, the material removal rate obtained was low while the tool wear was higher.

Yan et al [24] studied the cutting of Al2O3 reinforced Al-6061 matrix through rotary electro-discharge machining with a disk-shaped electrode with Tagauchi methodology. A greater material removal rate was obtained due to the efficient debris deposal effect of the rotary disk electrode. It was inferred through Taguchi methodology that in general electrical parameters (Peak Current, Pulse duration, and Gap voltage) affect the machining characteristics (material removal rate, electrode wear rate & SR) more significantly than the non-electrical parameters (speed of rotational disc).

It is important to note that the machining of metal matrix composites using conventional machining processes causes the deterioration of surface quality due to the delamination between the ductile matrix, and hard and brittle reinforcement materials. Therefore, researchers around the world [44,50] were focusing on machining the MMCs after utilizing unconventional machining processes. In the present study, the authors attempted to investigate the effect of electrode material on the performance of electric discharge machining of aluminum MMCs. The novelty of the present work is the use of four different electrodes to estimate the MRR, TWR, and surface roughness during the machining of the fabricated Al-based MMC sample. Moreover, a comparative analysis was conducted to suggest the best electrode material that enhances the machining performance of the fabricated MMC during roughing and finishing operations which has not been done so far.

2. EXPERIMENTAL DETAILS

2.1 Materials

Bayer's red mud and TiC of 24 µm and 300 µm mesh size respectively are used as particulate reinforcements. The chemical compositions of Bayer red mud and specifications of TiC are presented in Tables 1 & 2. Bayer red mud particle size ranges between 0.8-50 micrometers with an average value of 14.8 micrometers. The density of Bayer red mud is 2.70 g/cc [26].

Table 1. Showing specifications of TiC [48].

Molar Mass (g/mol)	59.89
Density (g/cm^3)	4.9-5.2
Solubility in Water	Insoluble
ICSC number	1319
Boiling Point (^{o}C)	4820
Surface Area (m^2/g)	10
Thermal Conductivity at 20^{o}C	0.041
Crystallography	Cubic Crystalline
Color	Light Grey

TiC depicts several properties such as high hardness, elastic modulus, and thermal conductivity along with low density that make it an appropriate reinforcement for aluminum metal matrix [27,28].

Wettability and reactivity of TiC are important qualities required for reinforcement and matrix adhesion which greatly influences the final properties of the composite as these parameters affect the load transfer from matrix to reinforcements [29,30]. The density of titanium carbide powder is 4.93 g/cc [31].

Table 2. Showing chemical composition in red mud.

Compound	Fe_2O_3	Al_2O_3	SiO_2
Wt. fraction	30-60%	10-20%	3-50%
Compound	Na_2O	CaO	TiO_2
Wt. fraction	2-10%	2-8%	Trace-25%

A356 is used as matrix material. A356 has been shown to have good mechanical and wear characteristics at room temperature. It also has improved mechanical properties at higher temperatures. It solidifies in a wide range of temperature intervals within solidus and liquidus temperatures making it favourable as a matrix for composite manufacture using composting [32]. The composition of A356 aluminum alloy is presented in Table 3. The density of A356 is 2.67 g/cc. It has a solidus temperature of 556 °C and a liquidus temperature of 616 °C. Its pouring temperature is 680 °C [34]. In the present study, AMMC is fabricated with the addition of 15 vol% of red mud and 12 vol% of TiC into the matrix A356 [49].

Table 3. Showing alloying elements of A356.

Compound	Standard wt% [33]	As received Wt%
Al	90-93	91
Si	6-7.5	7.2
Mg	0.45	0.44
Cu	0.25	0.25
Mn	0.35	0.35
Fe	0.6	0.6
Ti	0.25	0.25
Zn	0.35	0.35

The percentages were chosen in accordance with previous studies [35,36]. The die used for the composite fabrication is rectangular shaped made of cast iron. The size of the die cavity is (10 x 6 x 5) mm^3.

2.2 Fabrication of composite

For the fabrication of the castings, a mild steel rectangular die set of 120 X 50 X 5 mm^3 has been utilized. The die was clamped and preheated to 300 °C [37] for six hours to avoid casting defects. The required amount of red mud and titanium carbide was weighed and kept aside. A weighed amount of A356 alloy is placed in a graphite crucible for melting the alloy inside an electric pit furnace. The furnace temperature was set at 750 °C, greater than the melting temperature of A356 to superheat the melt. Red mud was preheated to 500 °C for 15 minutes [35]. Preheating of reinforcements is required to remove the entrapped moisture as well as not to lower the temperature of the molten matrix while adding the reinforcements. TiC was preheated at 300 °C [38]. Red mud was added into the melt and mechanically stirred at 400rpm for 1 minute followed by the addition of TiC under the same stirring conditions. Then the molten metal matrix is put into the preheated die cavity and allowed to cool to room temperature forming a solid metal matrix. After cooling, the die was un-clamped and the cast specimen was then ejected from the die for further experimentation. Fig. 1 shows the die and the stir cast component fabricated.

Fig. 1. Photograph of fabricated hybrid composite with die.

2.3 Electric discharge machining of A356/ Red mud/TiC hybrid composite

The microstructural and mechanical characterization of the fabricated aluminum red mud composite was presented in Ref. [49]. Further, in the present manuscript, the authors investigated the machining performance of the said composites. Fig. 2 shows the schematic of electro-discharge machining. Further, the Electro-discharge machining working principle is based upon the erosion of unwanted material by melting followed by vaporizing. The electrical energy required for erosion is supplied to the tool electrode which acts as a negative electrode while the work material acts as a positive electrode. The cathode and the anode are separated by a small spark gap in which discharge occurs causing sparks. These sparks result in the erosion of work material. The electrodes are immersed into a dielectric medium which is required for flushing of removed material as well as to restore the potential difference after breakdown such that a new dielectric breakdown can occur.

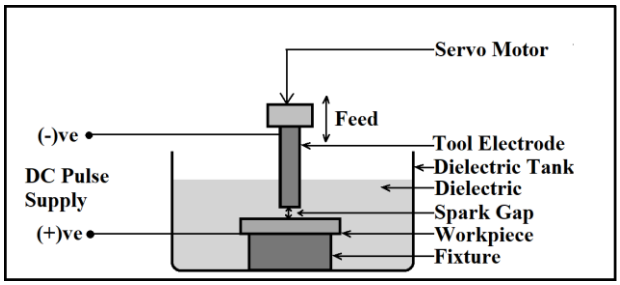

Fig. 2. Schematic diagram of electro-discharge machining process,

Table 4. Showing the EDM settings [46],

Frequency	50Hz
Dielectric	EDM Oil (relative density 0.763 g/cc)
Electrode material	brass, copper, graphite, stainless steel
Diameter of electrode	8mm
Gap Voltage, V_g	50, 100 volts
Peak Voltage, I_p	6 Amp
Pulse on time, T_{on}	40, 50, 60 µs
Depth of Cut	5mm
Maximum Flushing Pressure	10MPa

Fig. 2 shows the electro-discharge machining process schematic. The EDM studies are carried out in ELECTRONICA–SMART ZNC EDM machines. The parameters chosen for the series of experiments are given in Table 4. The six sets of experiments were carried out according to the input response levels of peak current, pulse on time, and gap voltage using different electrodes viz. Brass (B), Copper (C), Graphite (G), and Stainless Steel (S) as given in Table 5.

Table 5. Level of Input Process Parameters.

Machining Parameters	1	2	3	4	5	6
Peak current, Ip (in Amp)	10	6	6	6	10	10
Pulse on time, Ton (in µs)	40	60	50	50	50	50
Gap voltage, Vg (in volts)	100	50	50	100	50	100

Fig. 3-a-b shows the different material electrodes and the corresponding impression created during electric discharge machining.

The material removal rate (MRR) is mathematically calculated according to Eq (1).

$$MRR = (W_b - W_a) / t \quad (1)$$

Here, W_b and W_a represent the weight of the workpiece before and after machining respectively and t represents the machining time.

Tool Wear Rate (TWR) is obtained according to Eq (2) given below.

$$TWR = (T_b - T_a) / t \quad (2)$$

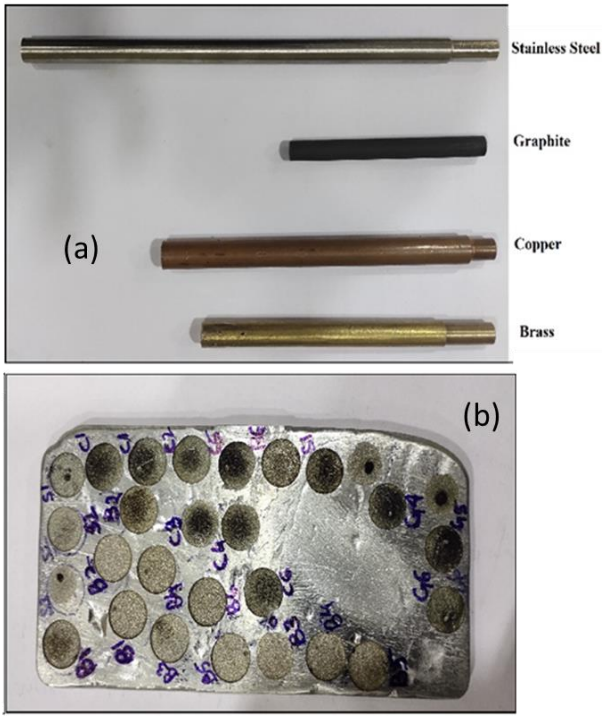

Fig. 3. Photograph showing (a) Types of electrode used; (b) Impressions created during EDM.

Here, T_b and T_a represent the weight of the electrode before and after machining respectively and t represents the machining time. Fig. 4 The EDM used for the experiment and the process of creating the impression.

Fig. 4. Photograph showing (a) EDM machine; (b) Impressions being created during EDM.

2.4 Surface roughness

Surface Roughness is measured using the Mitutoyo Surftest SV2100 M4 tester as shown in the fig. 5. It uses a stylus method of measurement and can measure roughness up to 500 µm.

Fig. 5. Photograph showing Surface roughness tester.

The pin of the tester moves from left to right in the impression to obtain the R_{a1} value and similarly moves from right to left in the impression to obtain the R_{a2} value.

The average of R_{a1} and R_{a2} gives the surface roughness average R_a.

3. RESULTS AND DISCUSSION

3.1 Material removal rate

Experimental studies according to input labels described in Table 4 have been carried out to depict the influence of the different electrodes on the material removal rate. The points on the X-axis denote the experimental conditions mentioned in Table 4 for each electrode i.e. brass (B), copper (C), Graphite (G), and stainless steel (S). MRR is calculated using Eq. (1). The material removal rate is plotted in Fig. 6 .

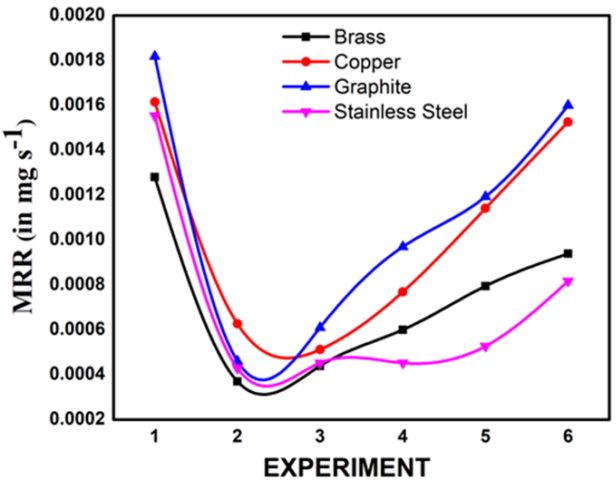

Fig. 6. Plot showing the comparison of MRR with various electrodes.

MRR depends on the electrode material, workpiece material dielectric flushing, and frequency of sparks. With a greater frequency of sparks, improper removal of stock occurs. With an increase in peak current MRR increases, as with an increase in peak current, discharge energy also increases. There is no significant increase in MMR due to the use of brass electrodes. However, due to machining with brass electrodes, a thin layer of tool material gets adhered to the workpiece. For Copper electrodes higher discharge current leads to higher MRR. This is because the increased spark discharge energy leads to an impulsive force in the spark gap which facilitates the melting and vaporization of work piece material [46]. MRR with graphite electrodes is much higher compared to copper and brass electrodes and several times higher than stainless steel electrodes. Similar findings were also reported [45].

MRR also increases with increases in pulse on time. As Ton increases the spark energy also increases which leads to more material removal. Also, with an increase in gap voltage Vg, the material removal rate increases for electrodes due to an increase in spark energy. For brass electrodes, MRR initially increases and then starts to fall off as increased Vg causes harsh concentrated discharge [25]. Material removal rates are found to be similar for copper and graphite electrodes. For a level with a higher peak current, the amount of loss of mass is also higher. Similar studies were also reported by Haron et al [39] while studying the performance of Cu and graphite electrodes during EDM of XW42 tool steel.

3.2 Tool wear rate

The points on the X-axis denote the experimental conditions mentioned in Table 4 for each electrode i.e. brass (B), copper (C), Graphite (G), and stainless steel (S).

TWR is calculated using Eq. (2). The tool wear rate for different electrode materials were plotted in Fig. 7.

Tool wear is found to be a similar trend for copper and graphite electrodes. For a level with a higher peak current, the amount of loss of mass is also higher. Similar studies were also reported for TWR by Haron et al [39] while studying the performance of Cu and graphite electrodes during EDM of XW42 tool steel.

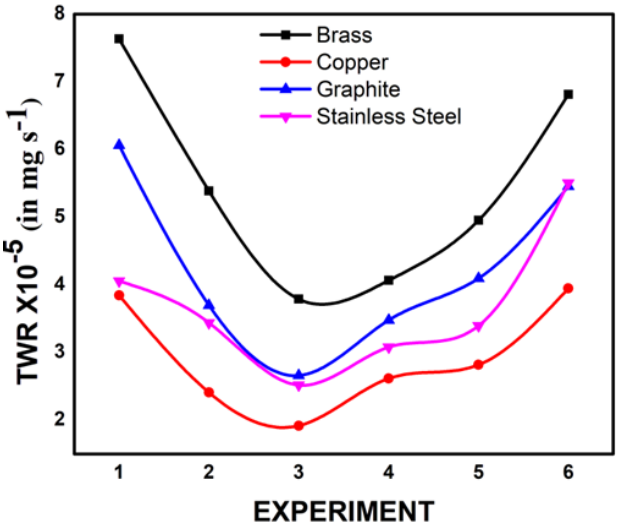

Fig. 7. Plot showing the comparison of TWR of various electrodes.

Tool wear in copper is found to be low while that of brass electrodes is more with an increase in discharge current. This may be due to the reason that the electrons from the workpiece (negative terminal) strike the tool surface (positive terminal) in the reverse polarity during EDM machining. These continuous strikes liberate greater energy on the tool surface and the tool materials with lower melting points wear more. Electrode wear is a cumulative result of high-density electron impact (electrical) and associated thermal effect; mechanical vibrations due to metal particles from workpieces; also due to irregularity in the microstructure of tool material [40]. The rate of brass electrode wear is higher than copper electrode which is again much higher than stainless steel electrode. Suhardjono [41] while machining hardened tool steel SKD 11 found that for 20A pulse current, the wear rate of brass is about four times the wear rate of copper and about six times the wear rate of stainless steel electrode which further increases with an increase in pulse current. Tool wear of graphite is significantly lower than brass electrodes which can be attributed to the large difference in their melting points. F. Wang et al. [42] and H.M. Chow et al. [43] in their EDM studies reported that melting at elevated temperatures is the main process in which materials are removed during arc machining due to the low melting point of the tool material will result in high tool wear rate.

3.3 Surface roughness

The surface roughness values obtained using the Mitutoyo Surftest SV2100 M4 tester are plotted in the graph shown in the figure. These values are plotted in the graph shown in Figure 8. Stainless steel electrode produces the best surface finish amongst the chosen copper, graphite, and brass electrodes. H. Singh and A. Singh [44] while studying the surface roughness produced during EDM with brass and copper electrodes also reported similar results for brass electrodes. With high MRR, larger and deeper craters are formed causing poor surface finish. This can be associated with the resulting rougher surfaces of graphite and copper electrodes. EDM with brass electrodes causes only a low rate of increase in surface roughness against discharge current and forms smaller craters resulting in lower surface roughness [45].

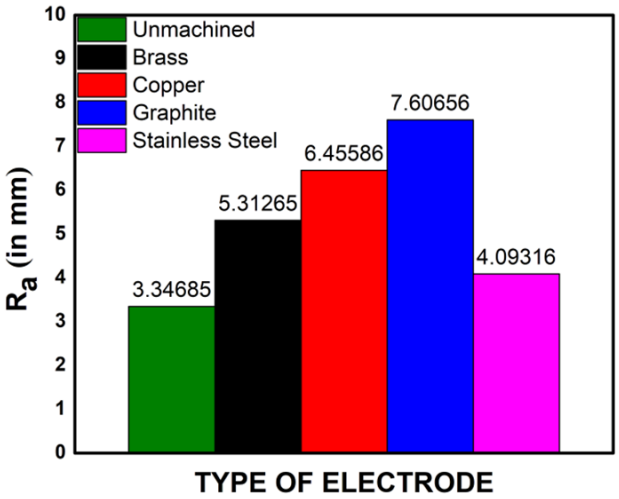

Fig. 8. Plot showing the comparison of surface roughness between different electrode materials.

Irrespective of the type of electrode used, the surface finish decreases with an increase in current. Analysis of surface roughness shows that graphite produces the poorest surface. This is because of the porous and coarse grain structure of graphite electrodes.

As EDM is a copying process, the open-grain structure of the graphite electrode gets imprinted onto the workpiece. The Cu electrode produces a better surface than the graphite electrode because of its better electrical and thermal properties than graphite. Good electrical conductivity leads to uniform and sustainable pulse discharges thus diminishing the chances of short circuits and arcing. It can be concluded that for a better-finished surface, there must be high frequency and low amperage current [46]. Similar results were also obtained by Lonardo et al. [47] and S. Singh et al. [40] while machining with copper electrodes.

4. CONCLUSION

The electric discharge machining of the A356 hybrid MMC has been conducted in the present study. From the experimental investigations on the machining of hybrid MMC using EDM, MRR, TWR, and SR are obtained for different electrode materials namely brass, copper, graphite, and stainless steel. The experimental results of EDM machining of hybrid MMC show that MRR is higher for graphite electrodes followed by copper and brass electrodes. It is also observed that the MRR obtained is lowest for stainless steel electrodes for the present workpiece material. Further, tool wear is found to be low for stainless steel followed by copper and graphite electrodes while brass electrode shows a higher tool wear rate [50] during machining of A356/Red mud/TiC composite. Graphite had shown a 57.19% improvement in MRR when compared with stainless steel which had produced a low value of MRR. Further, stainless steel has shown a 90.73% reduction in TWR when compared with brass which has shown a high value of TWR. It is also found that the stainless-steel electrode is found to give a better surface finish than brass, graphite, and copper electrodes. After considering the multiple responses, namely MRR, TWR, and surface roughness, the combination of aluminum MMC workpiece and stainless-steel tool has given the lowest value of the surface roughness, and tool wear rate with a comparable value of MRR when compared with the other combination of workpiece and tool materials. It is also important to note that Graphite electrodes followed by copper and brass electrodes can be utilized for roughing operations while stainless steel electrode is used for finishing operations.

REFERENCES

[1] K. K. Chawla, Composite materials. 2012, doi: 10.1007/978-0-387-74365-3.

[2] X. Sun, Y. Han, S. Cao, P. Qiu, and W. Lu, "Rapid in-situ reaction synthesis of novel TiC and carbon nanotubes reinforced titanium matrix composites," *Journal of Materials Science and Technology/Journal of Materials Science & Technology*, vol. 33, no. 10, pp. 1165–1171, Oct. 2017, doi: 10.1016/j.jmst.2017.07.005.

[3] M. Razavi, R. Ghaderi, M. R. Rahimipour, and M. O. Shabani, "Effect of addition of TIC Master Alloy on the properties of CK45," *Materials and Manufacturing Processes*, vol. 28, no. 1, pp. 31–35, Dec. 2012, doi: 10.1080/10426914.2012.677916.

[4] M. Razavi, R. Ghaderi, M. R. Rahimipour, and M. O. Shabni, "Synthesis of TIC Master alloy in nanometer scale by mechanical milling," *Materials and Manufacturing Processes*, vol. 27, no. 12, pp. 1310–1314, Dec. 2012, doi: 10.1080/10426914.2012.663142.

[5] F. Saba, S. A. Sajjadi, M. Haddad-Sabzevar, and F. Zhang, "TiC-modified carbon nanotubes, TiC nanotubes and TiC nanorods: Synthesis and characterization," *Ceramics International*, vol. 44, no. 7, pp. 7949–7954, May 2018, doi: 10.1016/j.ceramint.2018.01.233.

[6] H. A. Rastegari, S. Asgari, and S. M. Abbasi, "Producing Ti–6Al–4V/TiC composite with good ductility by vacuum induction melting furnace and hot rolling process," *Materials in Engineering*, vol. 32, no. 10, pp. 5010–5014, Dec. 2011, doi: 10.1016/j.matdes.2011.06.009.

[7] K. R. Kumar, K. Kiran, and V. S. Sreebalaji, "Micro structural characteristics and mechanical behaviour of aluminium matrix composites reinforced with titanium carbide," *Journal of Alloys and Compounds*, vol. 723, pp. 795–801, Nov. 2017, doi: 10.1016/j.jallcom.2017.06.309.

[8] J. Hashim, L. Looney, and M. S. J. Hashmi, "Particle distribution in cast metal matrix composites—Part II," *Journal of Materials Processing Technology*, vol. 123, no. 2, pp. 258–263, Apr. 2002, doi: 10.1016/s0924-0136(02)00099-7.

[9] H. S. Vaziri, A. Shokuhfar, and S. S. S. Afghahi, "Investigation of mechanical and tribological properties of aluminum reinforced with tungsten disulfide (WS2) nanoparticles," *Materials Research Express*, vol. 6, no. 4, p. 045018, Jan. 2019, doi: 10.1088/2053-1591/aafa00.

[10] C. Nazık, N. Tarakçıoğlu, S. Özkaya, F. Erdemır, and A. Çanakçı, "Determination of effect of B4C content on density and tensile strength of AA7075/ B4C composite produced via powder technology," *International Journal of Materials, Mechanics and Manufacturing*, pp. 251–254, Jan. 2015, doi: 10.18178/ijmmm.2016.4.4.266.

[11] M. L. T. Guo and Chi. -y. A. Tsao, "Tribological behavior of aluminum/SiC/nickel-coated graphite hybrid composites," *Materials Science and Engineering. A, Structural Materials: Properties, Microstructures and Processing/ Materials Science & Engineering. A, Structural Materials: Properties, Microstructure and Processing*, vol. 333, no. 1–2, pp. 134–145, Aug. 2002, doi: 10.1016/s0921-5093(01)01817-2.

[12] B. C. Pai and P. K. Rohatgi, "Production of cast aluminium-graphite particle composites using a pellet method," *Journal of Materials Science*, vol. 13, no. 2, pp. 329–335, Feb. 1978, doi: 10.1007/bf00647777.

[13] J. Zhang, R. J. Perez, and E. J. Lavernia, "Effect of SiC and graphite particulates on the damping behavior of metal matrix composites," *Acta Metallurgica Et Materialia*, vol. 42, no. 2, pp. 395–409, Feb. 1994, doi: 10.1016/0956-7151(94) 90495-2.

[14] S. Kant, A. S. Verma, Research India Publications, and Department of Production & Industrial Engineering, PEC University of Technology, Chandigarh, "Stir casting process in particulate aluminium metal Matrix Composite: A review," *International Journal of Mechanics and Solids,* vol. 12, no. 1, pp. 61–69, 2017.

[15] C.Saravanan, K.Subramanian, V.Krishnan, and R.Narayanan, *Effect of Particulate Reinforced Aluminium Metal Matrix Composite*, Mechanics and Mechanical Engineering, 2015.

[16] K. Kalaiselvan, N. Murugan, and S. Parameswaran, "Production and characterization of AA6061–B_4C stir cast composite," *Materials in Engineering*, vol. 32, no. 7, pp. 4004–4009, Aug. 2011, doi: 10.1016/j.matdes.2011.03.018.

[17] B. S. Yigezu, P. K. Jha, and M. M. Mahapatra, "The Key Attributes of Synthesizing Ceramic Particulate Reinforced Al-Based Matrix Composites through Stir Casting Process: A Review," *Materials and Manufacturing Processes*, vol. 28, no. 9, pp. 969–979, Sep. 2013, doi: 10.1080/10426914.2012.677909.

[18] S. J. James, K. Venkatesan, P. Kuppan, and R. Ramanujam, "Hybrid Aluminium Metal Matrix Composite Reinforced with SiC and TiB2," *Procedia Engineering*, vol. 97, pp. 1018–1026, Jan. 2014, doi: 10.1016/j.proeng.2014.12.379.

[19] F. Müller and J. Monaghan, "Non-conventional machining of particle reinforced metal matrix composites," *Journal of Materials Processing Technology*, vol. 118, no. 1–3, pp. 278–285, Dec. 2001, doi: 10.1016/s0924-0136(01)00941-4.

[20] R C Naikar, "Characterization of al-red mud composite using stir casting method," *International Journal for Research in Applied Science and Engineering Technology*, vol. 5, no. 11, pp. 104–108, 2017.

[21] Amit Sharma, Sanjeev Kumar, and PEC University of Technology, Chandigarh, India, "Evaluation of red mud reinforced AL-2024 MMC fabricated using stir casting technique,"*Journal of Civil Engineering and Environmental Technology.*, vol. 3, pp. 193-197, 2016.

[22] R. Snoeys, F. Staelens, and W. Dekeyser, "Current trends in Non-Conventional Material Removal Processes," *CIRP Annals*, vol. 35, no. 2, pp. 467–480, Jan. 1986, doi: 10.1016/s0007-8506(07)60195-4.

[23] F. Müller and J. Monaghan, "Electro Discharge Machining of Particle Reinforced Metal Matrix Composites," in *A. K. Kochhar et al. (eds.), Proceedings of the Thirty-Second International Matador Conference*, pp. 425–430, 1997, doi: 10.1007/978-1-349-14620-8_67.

[24] B. H. Yan, C. C. Wang, W. D. Liu, and F. Y. Huang, "Machining Characteristics of Al 2 O 3 /6061Al Composite using Rotary EDM with a Disklike Electrode," *The International Journal of Advanced Manufacturing Technology*, vol. 16, no. 5, pp. 322–333, Apr. 2000, doi: 10.1007/s001700050164.

[25] M. A. Khairul, J. Zanganeh, and B. Moghtaderi, "The composition, recycling and utilisation of Bayer red mud," *Resources, Conservation and Recycling*, vol. 141, pp. 483–498, Feb. 2019, doi: 10.1016/j.resconrec.2018.11.006.

[26] P. Wang and D.-Y. Liu, "Physical and chemical properties of sintering red mud and bayer red mud and the implications for beneficial utilization," *Materials*, vol. 5, no. 10, pp. 1800–1810, Oct. 2012, doi: 10.3390/ma5101800.

[27] S. Sheibani and M. Fazel. Najafabadi, "In situ fabrication of Al–TiC Metal Matrix Composites by reactive slag process," *Materials in Engineering*, vol. 28, no. 8, pp. 2373–2378, Jan. 2007, doi: 10.1016/j.matdes.2006.08.004.

[28] A. Rajabi, M. J. Ghazali, and A. R. Daud, "Chemical composition, microstructure and sintering temperature modifications on mechanical properties of TiC-based cermet – A review," *Materials in Engineering*, vol. 67, pp. 95–106, Feb. 2015, doi: 10.1016/j.matdes.2014.10.081.

[29] A. R. Kennedy and S. M. Wyatt, "The effect of processing on the mechanical properties and interfacial strength of aluminium/TiC MMCs," *Composites Science and Technology*, vol. 60, no. 2, pp. 307–314, Feb. 2000, doi: 10.1016/s0266-3538(99)00125-6.

[30] E. Ghasali, Y. Palizdar, A. Jam, H. Rajaei, and T. Ebadzadeh, "Effect of Al and Mo addition on phase formation, mechanical and microstructure properties of spark plasma sintered iron alloy," *Materials Today Communications*, vol. 13, pp. 221-231, Dec. 2017, doi:10.1016/j.mtcomm.2017.10.005.

[31] M. L, J. S. Reddy, and P. G. Mukunda, "Compaction sintering and characterization of TIC reinforced aluminum metal matrix composites," *SSRG International Journal of Mechanical Engineering*, vol. 4, no. 2, pp. 24–28, Feb. 2017, doi: 10.14445/23488360/ijme-v4i2p104.

[32] N. Natarajan, S. Vijayarangan, and I. Rajendran, "Wear behaviour of A356/25SiCp aluminium matrix composites sliding against automobile friction material," *Wear*, vol. 261, no. 7–8, pp. 812–822, Oct. 2006, doi: 10.1016/j.wear.2006. 01.011.

[33] Z. Mišković, I. Bobić, S. Tripković, A. Rac, and A. Vencl, "The structure and mechanical properties of an aluminium A356 alloy base composite with Al2O3 particle additions," *Tribology in Industry*, vol. 28, no. 3-4, pp. 23-27, 2006.

[34] A. H. Ahmad, S. Naher, and D. Brabazon, "The effect of direct thermal method, temperature and time on microstructure of a cast aluminum alloy," *Materials and Manufacturing Processes*, vol. 29, no. 2, pp. 134–139, Feb. 2014, doi: 10.1080/10426914.2013.822980.

[35] B. Geetha and K. Ganesan, "Experimental investigation on influence of particle size on mechanical properties and wear behaviour of A356-red mud metal matrix composite," *AIP Conference Proceedings*, Jan. 2019, doi: 10.1063/1.5117929.

[36] M. H. Shojaeefard, M. Akbari, P. Asadi, and A. Khalkhali, "The effect of reinforcement type on the microstructure, mechanical properties, and wear resistance of A356 matrix composites produced by FSP," *The International Journal of Advanced Manufacturing Technology*, vol. 91, no. 1–4, pp. 1391–1407, Dec. 2016, doi: 10.1007/s00170-016-9853-0.

[37] H. H. Kim, J. S. S. Babu, and C. G. Kang, "Fabrication of A356 aluminum alloy matrix composite with CNTs/Al2O3 hybrid reinforcements," *Materials Science and Engineering. A, Structural Materials: Properties, Microstructures and Processing/ Materials Science & Engineering. A, Structural Materials: Properties, Microstructure and Processing*, vol. 573, pp. 92–99, Jun. 2013, doi: 10.1016/j.msea.2013.02.041.

[38] U. Pandey, R. Purohit, P. Agarwal, S. K. Dhakad, and R. S. Rana, "Effect of TiC particles on the mechanical properties of aluminium alloy metal matrix composites (MMCs)," *Materials Today: Proceedings*, vol. 4, no. 4, pp. 5452–5460, Jan. 2017, doi: 10.1016/j.matpr.2017.05.057.

[39] C. H. C. Haron, J. A. Ghani, Y. Burhanuddin, Y. K. Seong, and C. Y. Swee, "Copper and graphite electrodes performance in electrical-discharge machining of XW42 tool steel," *Journal of Materials Processing Technology*, vol. 201, no. 1–3, pp. 570–573, May 2008, doi: 10.1016/j.jmatprotec.2007.11.285.

[40] S. Singh, S. Maheshwari, and P. C. Pandey, "Some investigations into the electric discharge machining of hardened tool steel using different electrode materials," *Journal of Materials Processing Technology*, vol. 149, no. 1–3, pp. 272–277, Jun. 2004, doi: 10.1016/j.jmatprotec.2003. 11.046.

[41] S. Suhardjono "Characteristics Of Electrode Materials On Machining Performance Of Tool Steel Skd11 With Edm Shinking," *ARPN Journal of Engineering and Applied Sciences,* vol. 11, no. 2, Jan. 2016.

[42] F. Wang, Y. Liu, Y. Zhang, Z. Tang, R. Ji, and C. Zheng, "Compound machining of titanium alloy by super high speed EDM milling and arc machining," *Journal of Materials Processing Technology*, vol. 214, no. 3, pp. 531–538, Mar. 2014, doi: 10.1016/j.jmatprotec.2013.10.015.

[43] C.-C. Wang, H.-M. Chow, L.-D. Yang, and C.-T. Lu, "Recast layer removal after electrical discharge machining via Taguchi analysis: A feasibility study," *Journal of Materials Processing Technology*, vol. 209, no. 8, pp. 4134–4140, Apr. 2009, doi: 10.1016/j.jmatprotec.2008.10.012.

[44] H. Singh and A. Singh, "Examination of surface roughness using different machining parameter in EDM," *International Journal of Modern Engineering Research (IJMER)*, vol. 2, no. 6, pp. 4478-4479, Nov. 2012.

[45] A. Erden and S. Bilgin, "Role of Impurities in Electric Discharge Machining," in *XXI IMTDR Conference, Swansea,* pp. 345–350, Jan. 1981, doi: 10.1007/978-1-349-05861-7_45.

[46] P. Kuppan, S. Narayanan, R. Oyyaravelu, and A. S. S. Balan, "Performance evaluation of electrode materials in electric discharge deep hole drilling of Inconel 718 Superalloy," *Procedia Engineering*, vol. 174, pp. 53–59, Jan. 2017, doi: 10.1016/j.proeng.2017.01.141.

[47] P. M. Lonardo and A. A. Bruzzone, "Effect of flushing and electrode material on die sinking EDM," *CIRP Annals*, vol. 48, no. 1, pp. 123–126, Jan. 1999, doi: 10.1016/s0007-8506(07)63146-1.

[48] M. Mhadhbi, "Titanium carbide: synthesis, properties and applications," *Brilliant Engineering*, vol. 2, no. 2, pp. 1–11, Aug. 2020, doi: 10.36937/ben.2021.002.001.

[49] C. Kar and B. Surekha, "Characterisation of aluminium metal matrix composites reinforced with titanium carbide and red mud," *Materials Research Innovations*, vol. 25, no. 2, pp. 67–75, Feb. 2020, doi: 10.1080/14328917.2020. 1735683.

[50] M. M. Bahgat, A. Y. Shash, M. Abd-Rabou, and I. S. El-Mahallawi, "Influence of process parameters in electrical discharge machining on H13 die steel," *Heliyon*, vol. 5, no. 6, p. e01813, Jun. 2019, doi: 10.1016/j.heliyon.2019.e01813.